DEPARTMENT OF THE INTERIOR
UNITED STATES GEOLOGICAL SURVEY

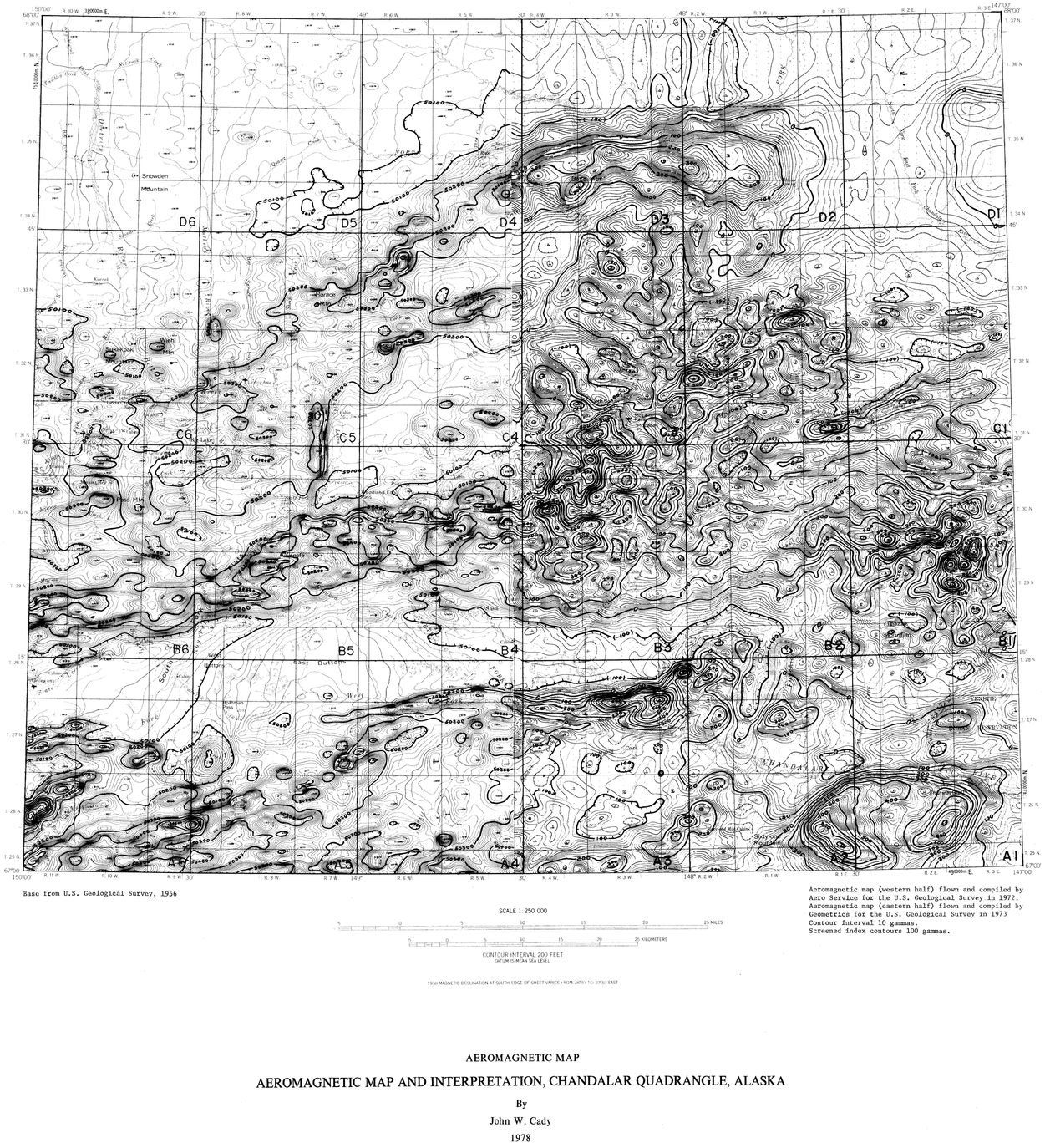

Base from U.S. Geological Survey, 1956

SCALE 1:250 000

CONTOUR INTERVAL 200 FEET
DATUM IS MEAN SEA LEVEL

1958 MAGNETIC DECLINATION AT SOUTH EDGE OF SHEET VARIES 1 FROM 30°E TO 33°E EAST

Aeromagnetic map (western half) flown and compiled by Aero Service for the U.S. Geological Survey in 1972.
Aeromagnetic map (eastern half) flown and compiled by Geometrics for the U.S. Geological Survey in 1973
Contour interval 10 gammas.
Screened index contours 100 gammas.

AEROMAGNETIC MAP

AEROMAGNETIC MAP AND INTERPRETATION, CHANDALAR QUADRANGLE, ALASKA

By

John W. Cady

1978

AEROMAGNETIC DATA

The aeromagnetic map of the Chandalar quadrangle was flown in two halves which were released as U.S. Geological Survey open-file reports in 1973 (western half) and 1974 (eastern half). The data were collected along north-south traverses spaced 2 km apart in the west and 1.6 km apart in the east. In the western half, a Doppler navigation system was controlled by 1:63,360 topographic mapping. In the eastern half, detailed topographic mapping was unavailable to control the Doppler navigation; hence undetected position errors may be present in the aeromagnetic map. Regional trends calculated from the 1965 International Geomagnetic Reference Field, updated to the times of survey, have been removed from both maps. In addition, a constant of 57,249.56 gammas was removed from the eastern half, yielding a residual map with negative gamma values in the lows; in the western half, however, a constant was not removed, so most anomaly values are above 50,000 gammas.

Topographic effects

The aircraft flew a nominal 300 m above the terrain. The radar altimetry data (where available in the eastern half of the quadrangle) show that the plane fell 75–150 m below the nominal elevation over mary ridges and flew 30–100 m above the nominal elevation in many valleys. A comparison of the aeromagnetic map with a topographic map, and an examination of selected magnetic and altimeter profiles shows, however, that no major false anomalies have been created by topography. In some places the topographic effect has made the crests of highs a little sharper over ridges and closed lows a little deeper over valleys. Several obvious cases have been noted by symbols on the interpretive map.

The correlation between valleys and aeromagnetic lows (in R. 3 W., T. 30–31 N.; R. 1 E. and R. 2–3 E., T. 29–30 N. (L2) on the interpretive map, was tested by 2½-dimensional magnetic modeling (Shuey and Pasquale, 1973; Cady, 1977) (figs. 1 and 2, Sheet 1). Figure 1 shows poor to fair correlation between the altimetry and aeromagnetic profiles. In figure 2, the two selected magnetic and altimeter profiles were chosen on the assumption that the aircraft flew at constant elevation and that the radar altimeter measured the changing elevation of the top of an aggravating 3 km thick magnetic body with a susceptibility of .025 x 10^{-3} cgs. (The thickness and susceptibility of the body were determined independently; see discussion of fig. 1.) The crosses correlate poorly with the observed profile, and the central low in the observed profile has far greater width than the topographic model would predict. This low, indicating a zone of low susceptibility, is discussed below.

In figure 2 the correlation between the altimetry and aeromagnetic profiles is poor, indicating a greater topographic effect. The crosses calculated for line 41 show that much of the aeromagnetic low can be explained by topography. In line 40, however, the full amplitude of the low is not reflected in the calculated crosses, and must be explained by a zone of low susceptibility discussed later. In figures 1 and 2 the magnetic datums are arbitrary, chosen by trial and error in an attempt to align the magnetic lows as much as possible by topography.

An interesting false high, labeled M6, occurs over the Dietrich River in R. 1 W., T. 33–34 N. Over magnetic terrains, false magnetic highs due to topography generally occur over ridges where the aircraft passes close to the magnetic rock. Flying up the gentle valley of the Dietrich River, however, the pilot would have had little difficulty maintaining a constant terrain clearance. Hence it was speculated that the 20–30 gamma anomaly over the Dietrich River was due to placer magnetite. Modeling, however, showed that magnetic sand in the river bed would produce a shorter-wavelength anomaly than is observed. Finally, calculations showed that if we varied the gradient of the Earth's main dipole field, increasing downward, is about 27 gammas per 1,000 m. In the northwest part of the Chandalar quadrangle, where the terrane is virtually nonmagnetic, this gradient dominates gradients due to near-surface magnetic rocks. Hence high M6 is caused by the aircraft flying 600–1,000 m lower in the Dietrich River valley than over the ridges to either side.

ROCK SUSCEPTIBILITIES

The aeromagnetic anomalies and patterns on the aeromagnetic map are caused by varying percentages of magnetic minerals, principally magnetite, in the underlying rocks. A first comparison of the geologic map (Brosgé and Reiser, 1964) and aeromagnetic maps suggests that the fossiliferous sedimentary rocks are very weakly magnetic (Q^s and Q^{gs}). Granitic intrusives range from weakly or nonmagnetic ($k \cdot 10^{-3}$ or 10^{-3}) to highly magnetic ($k \cdot 10^{-3}$). Metamorphic rocks show a similar range. High susceptibility in them can probably be attributed to mafic composition and contact metamorphism. Gabbros probably retain premetamorphic magnetite and are highly magnetic ($k \cdot 10^{-3}$).

Magnetic measurements on a limited suite of samples are in accord with inferences drawn from the aeromagnetic map. Brosgé and Conradi (1971) reported the following range of susceptibility, in igneous and metamorphic rocks from the Chandalar quadrangle: 3 samples of basalt and andesite, -1. to +91.x10^{-3} cgs; 10 samples of Cretaceous granitic rock, -1. to 67.5x10^{-3}, mean for igneous rocks 25.8x10^{-3}; 2 samples of greenstone, 378. and 638.x10^{-3}; 6 samples of mica schist, -1. to 5.x10^{-3}, mean for metamorphic rocks 4.3x10^{-3}.

In addition, a susceptibility bridge, with a field-type head intended to measure the susceptibility of outcrops in situ, was used to roughly estimate the susceptibility of 61 hand specimens, mainly schist, collected in the vicinity of aeromagnetic highs. The bridge was calibrated by measurements made on cores of known susceptibility. 2.54 cm in diameter and 2.54 cm long. Rough corrections were made for the mass of the test specimen. Fifty-seven of the samples had a range between -1.x10^{-3} and 41.x10^{-3} cgs, with a mean of 11.x10^{-3} cgs. The 4 most magnetic samples, with a range of 120. to 397.x10^{-3}, had a mean of 242.x10.

METHOD OF INTERPRETATION

A preliminary aeromagnetic interpretation map was made without referring to the mapped geology. Major aeromagnetic highs and lows or areas of low magnetic relief were identified on a colored copy of the aeromagnetic map. Most lows either coincide with broad areas of low magnetic relief bounded by highs, or occur in proximity to a high. In either case, the lows are normal polarization lows caused by the dipole nature of magnetic sources. There is no clear evidence that any lows on the map are caused by reverse remanent magnetization, although the north-south trending eastern portion of low LA may be such a case.

Initially, boundaries between magnetic and non-magnetic rock units were assumed to be vertical. They were drawn midway down the steepest main magnetic gradient bounding the highs. Subsequent analysis of anomaly shapes and magnetic modeling suggested that some of the boundaries are dipping. For a dipping boundary, the inferred surface intersection of the boundary is displaced updip from the steepest magnetic gradient. Inferred dips are shown by dip and strike symbols on the interpretation map.

The preliminary magnetic interpretation map was compared with the mapped geology and the inferred sources were correlated with mapped rock types. Inferred boundaries of magnetic units, especially the calc mica schist and the quartz mucovite schist, rarely coincide with mapped boundaries. This lack of coincidence is due partly to surficial cover and partly to variation of magnetite content within the rock units which is not reflected in the geologic mapping. Without geologic control on the surface intersection of magnetic boundaries, inferences about the dips of the boundaries are ambiguous. This ambiguity about dip could be rectified if surface gagnetometer profiles were used to locate the surface intersection of the magnetic boundaries. The surface magnetic profiling would also help to identify the rock type responsible for the anomalies.

MAGNETIC ROCK UNITS

Interpretation of the aeromagnetic map leads to a lumping together of certain rock units. For example, a large area defined by magnetic highs is labeled calcareous schist and marble and tactite (CSM) on the interpretation map even though it contains other rock types, because magnetic portions of the calcareous schist and tactite are interpreted to be the source of the high. Other rock units used as labels for magnetic highs, are quartz-mucovite schist (QMS), mafic rocks (MR), gabbroo (MRG), granite and migmatite (GR_1), and highly magnetic granite (GR_2). Nonmagnetic granite is labeled GR^n.

Calc-mica schist, marble and tactite, including calc-silicate hornfels (CSM)

This unit gives rise to a broad belt of magnetic highs (labeled H1) running from southwest to northeast across the northern half of the map. The unit forms an anticlinal sheath above less-magnetic granitic rocks which runs from T. 31 N., R. 10 W. east-northeast at least to T. 35 N., R. 1 W. The exposed granite core (gr) of the anticline is roughly marked by an area of low aeromagnetic relief. The northern flank of the anticline, in which a thick section of the calcareous schist is exposed, has a better developed aeromagnetic high than the south flank, where exposures of calcareous schist are patchy. The aeromagnetic high is best developed in the northeast over four Creek (T. 35 N., R. 2 W.) where the calcareous schists are covered by alluvium. It appears that the granite-cored anticline noses eastward, and, from Four Creek east, a thick prow-like wedge of CSM rocks occurs at depth, marked by the nose of the aeromagnetic high.

A saddle near T. 35 N., R. 2 E. separates the highs labeled H1 from a subdued high to the east labeled CSM?. A possible source for the high in the CSM? area is an eastward shallowing of the CSM anticline which plunges out west of the saddle. The CSM? high may indicate a deeply buried pluton, possibly in the core of the westward-plunging anticlinorium which is better exposed a few kilometers east of the Chandalar quadrangle.

Porphyry molybdenum and copper deposits are associated with the granite (gr) in the central part of the CSM anticline. Three thrust faults in T. 33 and 34 N., R. 6 W., and T. 33 N., R. 5 W., coincide in part with aeromagnetic highs. The faults are interesting because one of them (F1) lies in a zone of molybdenum geochemical anomalies and the other two (F2 and F3) lie in a zone of copper geochemical anomalies. If the faults are mineralized, and if they juxtapose a magnetic rock unit with a non-magnetic rock unit, surface or detailed aeromagnetic mapping may be a useful prospecting tool.

The specific rock type containing the magnetite in the CSM unit is unknown. The exposures of calcareous schist that are more than 5 km north of the granitic core of the anticline are lower greenschist grade and are unaccompanied by magnetic highs, whereas the bulk of the calcareous schist adjacent to the granitic core includes many areas of low pressure, high temperature hornfels, and is accompanied by magnetic highs. Hence, I infer that the magnetite occurs as a hornfels-grade metamorphic mineral.

The north-dipping magnetic contact zone of the CSM unit causes a normal magnetic polarization low labeled L1 over the non-magnetic Silurian to Upper Devonian Skajit limestone. Along this limestone belt there occurs a zone of geochemical anomalies and deposits of copper, lead, and zinc. Morad and Wilkes (1978) report the presence of magnetite in tactite (calc-silicate hornfels) within low L1 (T. 35 N., R. 5 W.) and also west of R1 (T. 33 N., R. 6 W.). The magnetite bodies are small (a few tens of meters in greatest dimension) and do not cause any magnetic highs on the aeromagnetic map. Detailed aeromagnetic surveying or surface magnetometer surveying might aid in delineating magnetite bodies and associated porphyry copper deposits.

A subdued pattern of isolated highs and lows (labeled CSM?) lies in T. 37 N., R. 8½ W., in line with H1, suggesting that the surface exposures of Skajit Limestone are underlain by a buried magnetic unit, probably CSM. In this area the tactite occurs close to the granite. More to the northeast, in low L2, the tactite lies farther from the granite. Low L3 occurs at a constant distance north of the inferred contact with the CSM, marking northward-dipping beds of limestone and tactite. Supposing that the mineral deposits and tactite formed as a sheath several kilometers away from the granite core of the anticline and outboard from the magnetic hornfels zone of the CSM; we may then infer that, in the area labeled CSM?, a downfaulted or otherwise lowered, northward-dipping block of the mineralized tactite-sheath gives rise to copper deposits and geochemical anomalies closer to the CSM high.

Quartz mucovite schist (QMS)

Rocks in the QMS unit give rise to the major band of highs (labeled H2) that runs from east to west just south of the center of the map. A limb of this band of highs (labeled H2') runs northeasterly from T. 30 N., R. 4 W.

Two profiles (P1 and P2, fig. 3) were modeled in an attempt to determine the attitude of the south boundary of the QMS unit. The magnetic gradient along this boundary is steepest in the west (P1) than in the east (P2), suggesting a transition from a north-dipping, vertical contact in the west to a south-dipping contact in the east. Modeling shows this qualitative interpretation to be ambiguous. Because the surface intersection of the contact is covered by sediments, no unique solution for the dip of the contact is possible. For example, profile P1 is satisfied by both a vertical contact and a contact dipping 53° north. (Two dip and strike symbols on P1, at the surface intersection of the projected boundary for each model.) The first solution found for profile P2 was a vertical contact, but it is not unique.

Magnetic highs do not occur over all parts of the QMS unit. The lows labeled L1' that lie within and adjacent to the northeast part of the QMS unit lie partly over the weakly or nonmagnetic Upper Devonian Hunt Fork Shale, but mainly over quartz mica schist and mafic greenschist. The weakly magnetic rocks north of high H2 and H2' and south of high H7 also include much quartz-mica schist. As most of the QMS unit lies in an area mapped as lower greenschist facies, metamorphic grade does not seem to be the factor determining its magnetic properties. Many of the highs over the central part of the QMS unit occur close to bodies of greenschist and greenstone within the quartz mica schist, but careful fieldwork with a ground magnetometer would be required to determine whether greenstone is the source of the anomalies. Evidently there is great inhomogeneity within the quartz mica schist which has not been reflected in the geologic mapping.

The magnetic properties of the QMS unit bear further investigation for the possible association of magnetic anomalies with economic mineral deposits. Just east of the center of the map an area of magnetic highs coincides with the Chandalar gold mining district, which contains steeply dipping quartz veins with gold, arsenopyrite, pyrite, sphalerite, and traces of stibnite, galena, chalcopyrite, and siderite. The contorted anomaly pattern suggests a source body which is complex in three dimensions. Figure 4 shows mapped faults, faults interpolated from aligned flanks of aeromagnetic highs, gold claims, and greenstone, at the same scale as the aeromagnetic map. Tipped structures and greenstone units in the Chandalar B3 quadrangle trend northeasterly, whereas several faults and folds in the southern part of the C3 quadrangle trend southeasterly. Both southeasterly and northeasterly trends may be reflected in the magnetic anomaly pattern in this area. The contorted anomaly pattern probably results from the intersection of northeast- and southeast-trending structures. One southeast-trending fault (F4) is also shown on the aeromagnetic interpretation map in the south part of the C3 quadrangle. The fault may mark the northeastern boundary of a magnetic high. It coincides with the mineralized shear zone at the Mikado gold mine near its southeastern end. This fault and others like it may be discoverable in detailed magnetic prospecting and could provide a locus for gold mineralization.

A deep magnetic low (labeled L4) occurs at the junction of Big Creek and Jay Creek just south of the gold mining area, within the QMS unit and adjacent to highs over the QMS unit. Although the deepest part of the low occurs over a deeply incised valley, suggesting a topographic effect, lobes of the low occur over ridges to the southeast, northwest, northeast, and southwest of the central low. Magnetic modeling of the low (see discussion of fig. 1, topographic effects) showed that it is caused, at least in part, by a zone of low susceptibility. The main streams of Big Creek and McLellan Creek approximately aline with the southeast-northeast lobes of the low, while Trilby Creek and the southeast flowing part of Big Creek, aline with the northwest-southeast lobes of the low. I speculatively interpret the low as the result of a hydrothermal alteration zone or shear zone in the otherwise magnetic QMS unit. It could have been fluids inferred from magnetic gradients in figure 4. A smaller anomaly occurs in Jay Creek adjacent to the low.

An interesting elongate low (L2) cuts from southwest to northeast across the QMS unit in T. 29–30 N., R. 2–3 E. It alines with two creeks and correlates in part with low topography. Magnetic modeling of the low (see discussion of fig. 1, topographic effects) shows that, although much of the low is a topographic effect, at least one profile (line 40, fig. 2) requires a zone of low susceptibility. Low L2 is worth investigating as it may indicate an altered fault or joint system which has low magnetic susceptibility and which has also eroded preferentially to form a valley. This prediction of an alteration zone is corroborated by the geochemistry, which shows anomalies along the zone in antimony, zinc, boron, nickel, and cobalt.

Minor saddles in the high on the QMS unit occur where the unit has been deeply eroded by the middle fork of the Chandalar River, Flat Creek, and Funchion Creek. These are not "topographic lows", but are lows caused by the replacement of magnetic rock by alluvium.

Granitic rocks, migmatite and contaminated granite (GR_1 and GR_2)

In the northern part of the map area, the granitic rocks (gr and $gr?$) are non-magnetic and accompanied by magnetic lows. In the southern part however, granitic rocks cause magnetic highs. In the southeastern corner a granitic pluton (GR_1) causes the highest amplitude (600 to 800 gamma) anomaly on the map.

The highest magnetic anomaly occurs near the borders of the pluton and a relative low labeled L5 occurs in the center. My favored explanation for the highs on the border of the pluton is zonation of the pluton, possibly caused by assimilation of mafic country rock. Alternatively, low L5 may be due to an altered, weakly magnetic core in an otherwise magnetic pluton. Figure 5 shows a magnetic model which reproduces the observed magnetic anomaly along profile P6 over the pluton. The north border of the pluton dips north at 60 to 70 degrees, and the core of the pluton is less magnetic than its borders. The south border of the pluton, which occurs south of the Chandalar quadrangle, is less abrupt than the north border. It is represented in the model by a thinning of the main pluton and the addition of a second magnetic body to the south.

Farther west, and separated from the highly magnetic pluton by a zone of biotite-garnet schist, is a large (96 km long within the map area) granitic pluton (GR_2) containing zones of migmatite or contaminated granite. Several magnetic highs occur within the granitic rock in proximity to mapped migmatite. Presumably a contaminated zone within the granitic rock adjacent to the migmatite is responsible for the magnetic highs. The relationship is not perfect, however, for several migmatite bodies are not accompanied by magnetic highs in the adjacent granite. The attitude of the pluton is difficult to determine due to interfering anomalies from the volcanic rock described below.

Mafic extrusive and intrusive rocks (MR) and probable gabbro (MRG)

The mafic volcanic rocks are accompanied by magnetic highs ranging in amplitude between 50 and 600 gammas. Exposures of the mafic rocks roughly parallels the north boundary of the large Mesozoic pluton (GR_2) near the southwest border of the map. A possible interpretation is that stratified volcanic rocks were arched upward over the intruding pluton and erosion has left an upturned belt of volcanics around the border of the pluton.

Elongate magnetic highs, probably caused by bedded volcanics in R. 5 and 6 W., T. 27 and 28 N., are shown in profiles P3 and P4 in figure 6, while higher amplitude anomalies in R. 2 and 3 W., T. 27 N. and 28 N. (profile P5) probably mark gabbro on ultramafic bodies. The asymmetry of the profiles could indicate south-dipping dike-like magnetic sources, but I conclude instead that the asymmetry is caused by a step-like transition from magnetic granitic rocks to the south and non-magnetic sedimentary rocks to the north. Superimposed upon the step-like transition anomaly is a more symmetrical high caused by vertical or steep north-dipping prisms of mafic rocks.

Magnetic lows or featureless areas

A zone of low magnetic intensity (L3) lies north of high H1 associated with the CSM unit. This low has typical relief of less than 10 gammas to 20 gammas, broken only by the 35 gamma topographic high (M6) over the Dietrich River. It is not clear from the contour map whether the minor relief in this low is due to variation in the magnetic properties of the sedimentary rocks exposed at the surface or to variations in the magnetic properties of basement rocks. The deepest parts of the low occur over the Skajit Limestone, but as the limestone occurs frequently where there is no pronounced low, there is no evidence that the Skajit Limestone is any less magnetic than its sedimentary neighbors. The deepest part of the low is interpreted as being a polarization low associated with the high over the CSM unit.

The lows over the QMS unit have been discussed in connection with the highs over that unit. The conclusion is that there is important heterogeneity of magnetite content within the QMS unit which is not represented on the geologic map.

A zone of low magnetic relief and low magnetic intensity that includes the linear low L4 and some discontinuous lows further east runs the width of the map at approximately lat 67°15'N, south of the magnetic quartz mica schist and north of the magnetic mafic volcanic rocks. The zone is part of a topographic low called the Kobuk Trench that bounds the south side of the Brooks Range (Granitz, 1960). Along L4 it contains exposures of Quaternary sediments underlain by phyllite and greenstone. Near the east side of the quadrangle, the zone includes a hilly terrain with exposures of nonmagnetic biotite staurolite schist and quartz mucovite schist. I interpret the low as a normal polarization low caused by the contrast between nonmagnetic rocks in the Kobuk Trench (Quaternary sedimentary rocks and phyllite) and extensive zones of magnetic rock to the north (quartz-mucovite schist) and south (migmatite and contaminated granite).

The zone of magnetic lows coincides approximately with a gravity high which is probably caused by mafic or intermediate metavolcanic rocks. The magnetic lows are probably caused by thick Quaternary cover and greenschist metamorphism of the volcanic rocks for, elsewhere along the south flank of the Brooks Range, magnetic and gravity highs coincide over a belt of upper Paleozoic marine volcanic rocks (Barnes, 1970, 1975).

Finally, a magnetic low in T. 27 N., R. 9 W. is too deep and too isolated from neighboring highs to be a polarization low associated with those highs. It probably indicates a nonmagnetic pluton ($gr?$) intruding country rock of slightly magnetic metavolcanics. A small granite exposure on the edge of the low may be an outcrop of the pluton. An antimony anomaly occurs in the vicinity.

SUMMARY AND CONCLUSIONS

Very complex variations of the magnetic field in the Chandalar quadrangle indicate significant variations in magnetite content of rocks exposed at the surface and also buried at depth.

The interpretive map (sheet 2) identifies magnetic rock units, many of which differ in their distribution from mapped geologic formations.

Among the rock units delineated by highs on the aeromagnetic map are: an anticline of contact-metamorphosed calc-mica schist; a highly complex and variable band of quartz mucovite schist; volcanic rocks associated with the Kobuk Trench; and granitic plutons south of the Kobuk Trench. In contrast to those south of the Trench, granitic rocks north of the Kobuk Trench are nonmagnetic. Magnetic mapping may help to delineate copper, molybdenum, lead, and iron deposits associated with the magnetic calc-mica schist and nonmagnetic granite and limestone. Detailed magnetic mapping may be useful in delineating faults which may control gold-bearing veins in the quartz mucovite schist. Two magnetic lows may mark nonmagnetic, possibly mineralized shear zones or alteration zones in the quartz mucovite schist.

MISCELLANEOUS FIELD STUDIES
MAP MF-878C
CHANDALAR QUAD., ALASKA
SHEET 1 OF 2

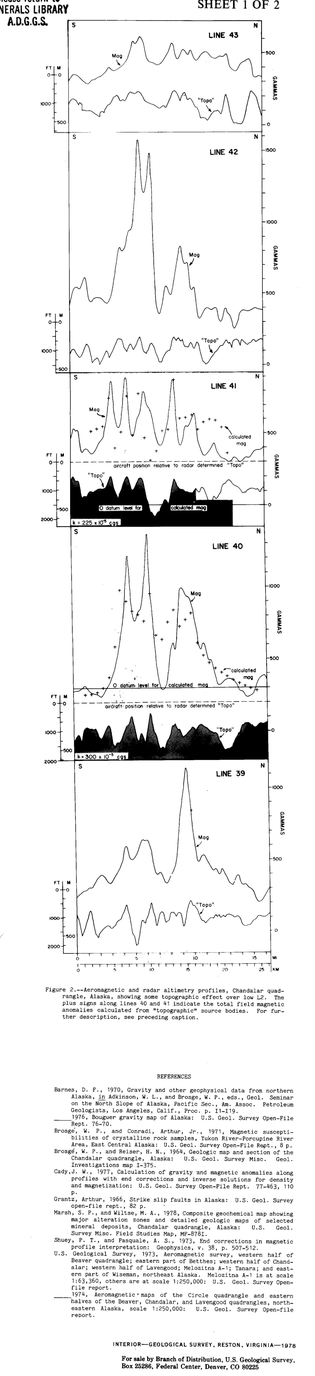

Figure 2.—Aeromagnetic and radar altimetry profiles, Chandalar quadrangle, Alaska, showing some topographic effect over low L2. The plus signs along lines 40 and 41 indicate the total field magnetic anomalies calculated from "topographic" source bodies. For further description, see preceding caption.

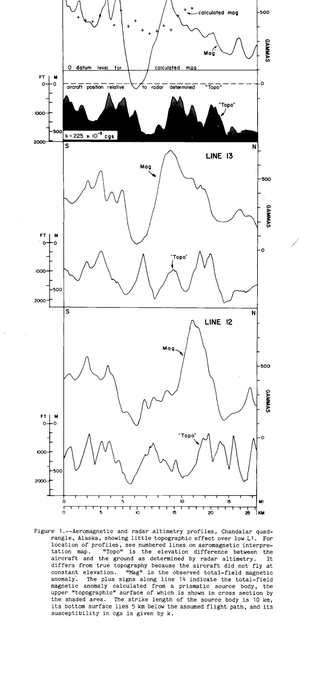

Figure 1.—Aeromagnetic and radar altimetry profiles, Chandalar quadrangle, Alaska, showing little topographic effect over low L1. For location of profiles, see numbered lines on aeromagnetic interpretation map. "Topo" is the elevation difference between the aircraft and the ground as determined by radar altimetry. It differs from true topography because the aircraft did not fly at constant elevation. "Mag" is the observed total-field magnetic anomaly. The plus signs along line 14 indicate the total-field magnetic anomaly calculated from a prismatic source body, the upper "topographic" surface of which is shown in cross section by the shaded area. The strike length of the source body is 10 km, its bottom surface lies 5 km below the assumed flight path, and its susceptibility in cgs is given by x.

REFERENCES

Barnes, D. F., 1970, Gravity and other geophysical data from northern Alaska, in Adkinson, W. L., and Brosgé, W. P., eds., Geol. Seminar on the North Slope of Alaska, Pacific Sec., Am. Assoc. Petroleum Geologists, Los Angeles, Calif., Proc. p. I1–I19.

———1975, Bouguer gravity map of Alaska: U.S. Geol. Survey Open-File Rept. 75–70.

Brosgé, W. P., and Conradi, Arthur, Jr., 1971, Magnetic susceptibilities of crystalline rock samples, Yukon River–Porcupine River area, East Central Alaska: U.S. Geol. Survey Open-File Rept., 8 p.

Brosgé, W. P., and Reiser, H. N., 1964, Geologic map and section of the Chandalar quadrangle, Alaska: U.S. Geol. Survey Misc. Geol. Investigations map I–375.

Cady, J. W., 1977, Calculation of gravity and magnetic anomalies along profiles with end corrections and inverse solutions for density and magnetization: U.S. Geol. Survey Open-File Report, 77–463, 110 p.

Granitz, Arthur, 1960, Zircon: slip faults in Alaska: U.S. Geol. Survey open-file rept., 82 p.

Marsh, S. P., and Wilkes, M. A., 1975, Composite geochemical map showing major alteration zones and detailed geologic maps of selected mineral deposits, Chandalar quadrangle, Alaska: U.S. Geol. Survey Misc. Field Studies Map, MF–878C.

Shuey, P. T., and Pasquale, A. S., 1973, End corrections in magnetic profile interpretation: Geophysics, v. 38, p. 507–512.

U.S. Geological Survey, 1973, Aeromagnetic survey, western half of Beaver quadrangle; eastern part of Bettles; western half of Chandalar; western half of Lavengood; Melozitna A–1; Tanana; and eastern part of Wiseman, northeast Alaska. Melozitna A–1 is at scale 1:63,360, others are at scale 1:250,000: U.S. Geol. Survey Open-file report.

———1974, Aeromagnetic maps of the Circle quadrangle and eastern halves of the Beaver, Chandalar, and Lavengood quadrangles, northeastern Alaska, scale 1:250,000: U.S. Geol. Survey Open-file report.

INTERIOR—GEOLOGICAL SURVEY, RESTON, VIRGINIA—1978

For sale by Branch of Distribution, U.S. Geological Survey, Box 25286, Federal Center, Denver, CO 80225